AFCRL-72-0418

LITHIUM-NICKEL SULFIDE BATTERIES

By

Lewis Gaines and Raymond Jasinski

Tyco Laboratories, Inc.
16 Hickory Drive
Waltham, Massachusetts 02154

Contract No. F19628-71-C-0153
Project No. 8659
Task No. 865904
Work Unit No. 86590401

FINAL REPORT

1 April 1971 - 31 March 1972

July 1972

Contractor Monitor: Richard Payne
Space Physics Laboratory

Approved for public release; distribution unlimited.

Prepared for

Air Force Cambridge Research Laboratories
Air Force Systems Command
United States Air Force
Bedford, Massachusetts 01730

Unclassified
Security Classification

DOCUMENT CONTROL DATA - R & D

(Security classification of title, body of abstract and indexing annotation must be entered when the overall report is classified)

1. ORIGINATING ACTIVITY (Corporate author)	2a. REPORT SECURITY CLASSIFICATION
Tyco Laboratories, Inc. 16 Hickory Drive Waltham, Massachusetts 02154	Unclassified 2b. GROUP

3. REPORT TITLE

LITHIUM-NICKEL SULFIDE BATTERIES

4. DESCRIPTIVE NOTES (Type of report and inclusive dates)

Final. Scientific 1 April 1971 - 31 March 1972 - Approved 9/1/72

5. AUTHOR(S) (First name, middle initial, last name)

Lewis Gaines
Raymond Jasinski

6. REPORT DATE	7a. TOTAL NO. OF PAGES	7b. NO. OF REFS
July 1972	44	None

8a. CONTRACT OR GRANT NO.	9a. ORIGINATOR'S REPORT NUMBER(S)
F19628-71-C-0153 b. PROJECT Task, Work Unit Nos. 8659-04-01 c. DoD Element 61102F d. DoD Subelement 681308	C929 9b. OTHER REPORT NO(S) (Any other numbers that may be assigned this report) AFCRL-72-0418

10. DISTRIBUTION STATEMENT

A - Approved for public release; distribution unlimited.

11. SUPPLEMENTARY NOTES	12. SPONSORING MILITARY ACTIVITY
Technical	Air Force Cambridge Research Laboratories (PH) L. G. Hanscom Field Bedford, Massachusetts 01730

13. ABSTRACT

Investigation of the high rate discharge performance of Ni_3S_2 indicated that rate capability was strongly influenced by the viscosity of the cell electrolyte. Stable discharges at up to 6 mA/cm^2 (equivalent to the 5-hr rate for an electrode of typical thickness) were obtained from Teflon-bonded electrodes in a tetrahydrofuran/$LiClO_4$ electrolyte. Coulombic efficiencies on the order of 50% of theoretical could be obtained at 3 mA/cm^2. Previous results with propylene carbonate and butyrolactone solutions indicated rate limitations in the vicinity of 0.5 to 1 mA/cm^2.

Study of the Ni_3S_2 oxidation procedure indicated that the optimum temperature for the production of the high voltage material was 325°C. X-ray diffraction analysis of the oxidized Ni_3S_2 indicated the presence of the relatively sulfer rich nickel sulfides: Ni_7S_6 and $NiS_{1.09}$. These materials possess higher theoretical energy densities than Ni_3S_2. This advantage is compromised by the difficulty of obtaining high coulombic efficiencies from insulating materials. Oxidation of Ni_3S_2 at temperatures above 400°C results in the formation of NiO.

A brief study of the discharge properties of metallic oxides, carbonates, and cyanides in propylene carbonate/$LiClO_4$ electrolyte indicated that although several of these materials exhibited acceptable discharge and voltage efficiencies, none were of sufficient interest to justify further development.

DD FORM 1 NOV 68 1473 REPLACES DD FORM 1473, 1 JAN 64, WHICH IS OBSOLETE FOR ARMY USE.

Unclassified
Security Classification

1A

14. KEY WORDS	LINK A		LINK B		LINK C	
	ROLE	WT	ROLE	WT	ROLE	WT
Batteries						
Lithium						
Nickel sulfide						
Organic electrolytes						
Oxides						
Carbonates						
Cyanides						

AFCRL-72-0418

LITHIUM-NICKEL SULFIDE BATTERIES

By

Lewis Gaines and Raymond Jasinski

Tyco Laboratories, Inc.
16 Hickory Drive
Waltham, Massachusetts 02154

Contract No. F19628-71-C-0153
Project No. 8659
Task No. 865904
Work Unit No. 86590401

FINAL REPORT

1 April 1971 - 31 March 1972

July 1972

Contractor Monitor: Richard Payne
Space Physics Laboratory

Prepared for

Air Force Cambridge Research Laboratories
Air Force Systems Command
United States Air Force
Bedford, Massachusetts 01730

ABSTRACT

Investigation of the high rate discharge performance of Ni_3S_2 indicated that rate capability was strongly influenced by the viscosity of the cell electrolyte. Stable discharges at up to 6 mA/cm^2 (equivalent to the 5-hr rate for an electrode of typical thickness) were obtained from Teflon-bonded electrodes in a tetrahydrofuran/$LiClO_4$ electrolyte. Coulombic efficiencies on the order of 50% of theoretical could be obtained at 3 mA/cm^2. Previous results with propylene carbonate and butyrolactone solutions indicated rate limitations in the vicinity of 0.5 to 1 mA/cm^2.

Study of the Ni_3S_2 oxidation procedure indicated that the optimum temperature for the production of the high voltage material was 325°C. X-ray diffraction analysis of the oxidized Ni_3S_2 indicated the presence of the relatively sulfur rich nickel sulfides: Ni_7S_6 and $NiS_{1.09}$. These materials possess higher theoretical energy densities than Ni_3S_2. This advantage is compromised by the difficulty of obtaining high coulombic efficiencies from insulating materials. Oxidation of Ni_3S_2 at temperatures above 400°C results in the formation of NiO.

A brief study of the discharge properties of metallic oxides, carbonates, and cyanides in propylene carbonate/$LiClO_4$ electrolyte indicated that although several of these materials exhibited acceptable discharge and voltage efficiencies, none were of sufficient interest to justify further development.

Table of Contents

List of Illustrations

List of Tables

1. SUMMARY

The work described in this final report represents a development program designed to improve the performance of the lithium-nickel sulfide battery system at high rates and/or at low temperatures. Preliminary studies first established the stability of the nickel sulfide material in a tetrahydrofuran (THF)/$LiClO_4$ electrolyte. The relatively low viscosity of this solution makes it a logical alternative to the previously used propylene carbonate (PC) and butyrolactone (BL) solutions. During this initial program phase, THF purification methods were developed (distillation, lithium pre-treatment, and electrochemical water removal) in order to insure stability of the electrolyte solution in the cell environment.

Initial testing of Ni_3S_2 electrodes in a THF/1 M $LiClO_4$ electrolyte indicated that the principal rate limitation lay within the positive electrode. At 3 mA/cm^2 (equivalent to a 10-hr discharge for a Ni_3S_2 electrode of typical thickness), stable discharges were obtained at ~1.2 V. Positive utilization was a strong function of electrode porosity ranging from 90% for electrodes pressed at 1.6 tons/$in.^2$ to 50% for denser electrodes pressed at 4 tons/$in.^2$. These results represent a substantial improvement over those that had been obtained with PC or BL electrolytes. In the particular case of butyrolactone, practical utilizations were obtainable only at rates limited to 0.5 to 1 mA/cm^2.

Teflon-bonded nickel sulfide electrodes were then prepared in an effort to increase electrode porosity and surface area without sacrificing the structural integrity of the electrode. These studies showed a further improvement in performance. For an electrode containing 30% Teflon and sintered for 30 min at 280°C, stable discharges were obtained at rates up to 6 mA/cm^2. Further studies showed that decreases in Teflon content to the 10% level could be made without significant sacrifice in rate capability.

These studies on electrode structure were supplemented by an investigation of the Ni_3S_2 oxidation process. This procedure, in which Ni_3S_2 is heated in air in

the vicinity of 350°C, was found to produce a material discharging at a cell voltage 300 to 400 mV higher than that obtained from pure Ni_3S_2. X-ray diffraction analysis showed that the oxidation produces significant quantities of the sulfur rich nickel sulfides: $NiS_{1.09}$ and Ni_7S_6. At 325°C (the optimum temperature), the coulombic capacity of the high voltage material represented ~40% of the useful capacity of the electrode. Attempts to increase this fraction by raising the temperature resulted in the degeneration of the electrode structure and the production of NiO.

In an attempt to develop alternative cathode material with intrinsically higher rate capabilities, a screening program was performed on metallic oxides, carbonates, and cyanides. In half-cell testing, the oxides and carbonates exhibited high polarizations from the thermodynamic values of the cell potential. In spite of this fact, several of the transition metal materials (CuO, NiO, $NiCO_3$, $CoCO_3$, and basic cupric carbonate) discharged with acceptable coulombic utilizations in PC/$LiClO_4$.

In the case of the cyanides, CuCN and AgCN were found to discharge with utilizations greater than 50% at voltages within 700 mV of their thermodynamic values. Full-cell testing of these materials indicated that their solubility properties were apparently analogous to those of the complexation phenomena exhibited by the transition metal chlorides. In view of the lower theoretical energy densities inherent in the cyanides, further development work on these materials is not recommended.

II. INTRODUCTION

Several organic electrolyte-lithium batteries have been developed to the state where energy densities approximating 100 Whr/lb have been demonstrated with fully-packaged prototypes. A few have also demonstrated reasonable shelf life. The lithium-nickel sulfide system falls into this category.

The next general goal to be reached is the realization of this attractive energy density at high rates and at low temperatures. At the present state of the art, "high rates" are defined as complete cell discharges in 10 hr or less (equivalent to 3 mA/cm^2 for positives of typical thickness); low temperatures are $\leq$-20°F.

Previous experience with the lithium-nickel sulfide battery has implied that the Ahr capacity at high rates was, in part, limited by a mass transport process within the electrolyte. The major limitations on cell voltage have been: (a) the thermodynamics of the cell reaction, and (b) the polarization at the positive. Again, prior experience has indicated that the cell voltage can be increased by chemical pretreatment of the nickel sulfide, i.e., by altering the chemical composition of the positive. Therefore, the initial approach to improving battery performance was:

1. Develop less viscous electrolytes capable of sustaining higher current densities,

2. Optimize the structure of the positive plate,

3. Evaluate improvements in capacity and potential of the positive via prior controlled oxidation.

III. ELECTROLYTE STUDIES

The Li/Ni_3S_2 couple is unique among practical non-aqueous battery systems in that the extremely low solubility of the positive material avoids many of the solvent-electrode interactions which compromise the usefulness of alternative systems with higher available energy densities. For many applications, however, high energy density and long shelf life must be complemented by attractive performance at relatively high rates (e.g., a complete discharge in 10 hr or less). Accordingly, an experimental program, designed to elucidate the rate limiting process for the cathodic discharge of Ni_3S_2 and to optimize both the electrode structure and the electrolyte system for high rate performance, was performed. As described below, the program first considered the solubility and stability of Ni_3S_2 (and oxidized Ni_3S_2) in several electrolyte solvents of relatively low viscosity. This phase was followed by the development of high rate electrode structures using a THF/$LiClO_4$ electrolyte.

A. Solubility Measurements

A colorimetric method for nickel was adopted from "Standard Methods for the Examination of Water and Waste Water." The analysis is based on the formation of a soluble colored complex between nickel and dimethylglyoxime in the presence of bromine. The calibration curve was formed from standard solutions of nickel sulfate in water. It was shown that the presence of 5 ml of THF, DME (dimethoxyethane), or pyridine in the initial sample aliquot did not alter the calibration curve. The absorbance readings (measured at 445 μm) were taken on a Bausch and Lomb Spectronic 20. Since the first instrumental scale reading is 0.01 absorbance, values below this are to be regarded as semi-quantitative. Sample blanks, e.g., THF not exposed to Ni_3S_2, were non-detectable (0.000).

The calibration data are summarized in Table I. When plotted out, the data yield a straight line passing through the origin.

Table I. Nickel Analysis Calibration

Concentration of Nickel, mg/100 ml	Absorbance
0.05	0.135
0.10	0.270
0.15	0.405
0.20	0.530
0.25	0.630

For each of the solubility determinations, solvent (or solvent + electrolyte) was added to excess Ni_3S_2. The mixture was then stirred for a minimum of 24 hr. After allowing the solid phase to settle out, the supernate was decanted and centrifuged. Liquid for analysis was withdrawn via a long, narrow-tip eye dropper while illuminating the sample tube with a high intensity lamp. This procedure was followed in order to avoid the presence of particulate Ni_3S_2 in the test liquid.

Results are summarized in Table II for Ni_3S_2 prepared in the normal fashion. In Table III are solubilities for Ni_3S_2 subjected to air oxidation at 325°C.

The solubilities of Ni_3S_2 in the pure solvents and in the THF/$LiClO_4$ solution are all sufficiently low. For comparison, the solubility of Ag_2O in KOH is of the order of 5×10^{-4} M. The relatively high value for the DME/$LiClO_4$ solution is somewhat surprising. In view of the low value found for the solvent itself, specific Ni^{++}·DME complexation would not be anticipated. Crystallization of 1M $LiClO_4$ in DME was often found as the sample was withdrawn for analysis, thus raising the possibility of Ni_3S_2 entrainment in a viscous solution. This solubility question must be explored further before DME can be recommended for use with this battery system.

Comparing Table III with Table II indicates that the "oxidized Ni_3S_2," as prepared, is somewhat less soluble than nonoxidized nickel sulfide. The chemistry of the oxidation step is described in Section IV.

The increase in solubility via the addition of lithium salt to the solvent may be real, reflecting a reaction of the following type:

$$Ni_3S_2 + 4LiClO_4 \rightarrow 2Li_2S + 2Ni(ClO_4)_2 + Ni \qquad (1)$$

More likely, trace water carried with the salt (and not removed by the molecular sieves) may solubilize the salt. For example, 2 ppm residual water is 10^{-4} mol/ℓ, substantially greater than a number of the solubilities observed.

Table II. Solubility of Ni_3S_2

Solution	Absorbance	Concentration of Ni^{++} g/ℓ	Concentration of Ni^{++} mol/ℓ
THF	0.001 0.002	$\sim 7.3 \times 10^{-5}$	$\sim 1.29 \times 10^{-6}$
DME	0.008 0.002 0.007 0.003 0.007	22.8×10^{-5}	3.87×10^{-6}
Pyridine	0.028 0.040 0.027	143×10^{-5}	25.8×10^{-6}
THF + $LiClO_4$ (1N)	0.019 0.028 0.038 0.047 0.042	220×10^{-5} (average)	22×10^{-6} (average)
DME + $LiClO_4$ (1N)	0.108 0.182 0.188	691×10^{-5}	118×10^{-6}
PC + $LiClO_4$ (1N)	0.017	63×10^{-5}	12×10^{-6}

Table III. Solubility of Ni_3S_2 (Oxidized)

Solution	Absorbance	Concentration of Ni^{++} g/ℓ	Concentration of Ni^{++} mol/ℓ
THF	0.004 0.008	$<14 \times 10^{-5}$	$<2.6 \times 10^{-6}$
DME	0.008 0.002	$<28 \times 10^{-5}$	$<5 \times 10^{-3}$
Pyridine	0.019 0.009 0.017	70×10^{-5}	13×10^{-6}
THF + $LiClO_4$ (1N)	0.002 0.000 0.001 0.005 0.005	10.4×10^{-5} (average)	1.95×10^{-6} (average)
DME + $LiClO_4$ (1N)	0.166 0.268 0.238 0.530 0.530	1338×10^{-5} (average)	248×10^{-6} (average)
PC + $LiClO_4$ (1N)	0.005	22×10^{-5}	3.2×10^{-6}

A brief study was made of the solubility of Ni_3S_2 in water. Ni_3S_2 was equilibrated with water and aliquots removed for analysis; these are the values listed in Table IV for "unwashed" nickel sulfide. For the "washed" samples, the Ni_3S_2 was first placed in a Buchner funnel, rinsed with 500 ml of water, and finally extracted with 10cc for analysis. The rationale behind this latter sequence was to wash out unreacted nickel sulfate and end up with a true evaluation of material solubility.

Table IV. Solubility of Ni_3S_2 in Water
(Ni_3S_2 Batch No. AS-1)

	Absorbance	
	Unwashed	Washed
Sample 1	0.265	0.003
Sample 2	0.285	0.068

Obviously, there is a decrease in apparent solubility via washing the sample. It should also be noted that the concentration of water-extractable nickel varied with the preparation. For example, the "unwashed" values of absorbance for batch No. 557-45 was 0.77. To pursue this matter further, a sample of batch AS-1 was placed in a Soxhlet extractor operated for 3 days. The extracted nickel sulfide gave an apparent nickel ion solubility of 7.3×10^{-4}, which is higher than anticipated for a transition metal sulfide.

Two additional facts must also be explained: (1) the addition of water to Ni_3S_2 generates the odor of H_2S, and (2) the Soxhlet extract contains significant quantities of nickel hydroxide. It would appear that nickel sulfide, as prepared, is somewhat unstable in the presence of water. The detailed resolution of this point is considered to be beyond the scope of this program. It is sufficient to have shown that:

1. The solubility of reduced and "oxidized" nickel sulfide, as prepared, is sufficiently low in THF for use of this solvent in battery development.

2. The solubility of Ni_3S_2 in pyridine may be too high (2.3×10^{-5}M) for practical application; the benefits of a preliminary extraction have not been evaluated.

3. The presence of water will increasc the solubility of as-preparcd nickel sulfide.

4. It appears that some nickel-containing compound in the nickel sulfide product is more soluble in water than the major component, but not soluble in THF.

The most obvious compound explaining item (4) is unreduced nickel sulfatc. Dried $NiSO_4$ was, therefore, cquilibrated with THF and PC. The solubilities are listed in Table V.

Table V. Solubility of $NiSO_4$

Solution	Absorbance
THF	0.000
	0.001
	0.005
	0.001
PC	0.001

Essentially, then, the solubility of $NiSO_4$ in THF and PC is at the limit-of-dctection of the analytical method.

This result suggests a battery based on the cell reaction:

$$2\,Li + NiSO_4 \rightleftharpoons Li_2SO_4 + Ni \qquad (2)$$

The standard-free energy change for the above reaction is -131 kcal/mole, giving a cell voltage of 2.87 V. The cell's theoretical energy density is 491 Whr/lb, based on an equivalent weight of 84 for the reactant. The discharge efficiency and polarization of $NiSO_4$ in aprotic solvents remains to be determined, however.

B. Preliminary Experiments Using Tetrathydrofuran-Based Electrolytes

1. Performance Capability

Thc half cell reactions for the Li/Ni_3S_2 system are:

$$Li \rightarrow Li^+ + e^- \qquad (3)$$

and, presumably:

$$Ni_3S_2 + 4Li^+ + 4e^- \rightarrow 2Li_2S + Ni^\circ \qquad (4)$$

As far as the electrolyte is concerned, Li^+ is injected at the negative, transported to the positive and removed from solution. The current delivered by the cell to the external circuit must also be carried across the electrolyte space. Eq. (5) describes the maximum current density which can be carried by a binary electrolyte considering only migration and diffusion:

$$i_L = \frac{nFDZ_1C}{\delta} \quad (1 + \frac{Z_1}{Z_2})$$

where

Z_1 and Z_2 = transference number for Li^+ and ClO_4^-, respectively. (5)

Using a diffusion coefficient of 5×10^{-6} cm^2/sec and an electrode separation of 0.1 cm, i_L for 1M $LiClO_4$ in THF calculates as 10 mA/cm^2.

An experimental estimate of i_L in THF was attempted by using the reaction:

$$Li^+ + e^- \rightarrow Li$$

to simulate the removal of lithium ion at the nickel sulfide positive. In the case of the anodic section, the use of a smooth electrode of relatively high capacity simplifies data interpretation by isolating the process of ion transport across the electrolyte space from transport processes within a pore structure. A major complicating feature is the dimensional and surface change resulting from lithium deposition at the cathode.

In order to separate these effects, the first experiments were designed to establish the level of polarization associated with these separate anodic and cathodic processes. The measurements were performed in a conventional three-compartment cell using a 1-cm square of lithium foil as the working electrode. Potentials versus a lithium reference electrode were recorded using a Luggin capillary placed adjacent to the working electrode. The overpotentials, taken after a minimum of 10 min at each current density, are shown in Table VI.

Neither Tafel nor linear behavior is observed over the c.d. range studied. Nevertheless, it is apparent that the polarizations associated with the lithium anode and cathode are small up to 10 mA/cm^2. The relatively low rate of increase in the overpotential associated with the cathodic reaction is most likely related to the greatly increased surface area resulting from the deposition of significant amounts of dendritic lithium as the experiment progressed.

Table VI. Potential-Current Dependence
(1M $LiClO_4$ in THF)

Current Density mA/cm^2	Potential, mV versus Li/Li^+
Anodic $Li - Li^+ + e^-$	
0.01	1.2
0.10	10.0
1.00	58.0
2.00	77.0
4.00	94.0
10.00	150.0
Cathodic $Li^+ + e^- - Li$	
0.01	-7.7
0.10	-23.0
4.00	-31.0
10.00	-40.0

To look at electrolyte mass transport effects in a practical battery configuration, the following cell was assembled:

$$Li/LiClO_4\ (1M)\ THF/Li$$

A 9-cm × 5-cm Li ribbon was folded in half around a Li plate 4 cm × 5 cm, wrapped with a single layer of non-woven polypropylene mat. The cell was then sealed in a plastic bag. The data shown in Table VII was taken after 15 min at each current density.

Table VII. Performance of Li/Li Cell
($1M\ LiClO_4$ in THF)

Current Density, mA/cm^2	Potential, mV
0.05	15
0.5	37
1.0	35
2.0	40
5.0	62
7.5	80
10.0	98
12.5	114

There are some obvious inconsistencies between the data in Table VII and Table VI; much of this inconsistency is probably experimental artifact. Nevertheless, it can be concluded from these results that the electrolyte is capable of carrying significant current densities at low polarizations.

Based on these encouraging results, two similar polyethylene bag cells were set up with Ni_3S_2 +5% Al positives on the center electrodes (16 cm^2/side). After saturation with $1M\ LiClO_4$/THF, each cell was discharged at $3mA/cm^2$ until the cell voltage dropped below 1.8V. This last procedure eliminates most of the residual water and other electroactive impurities. The test results, shown in Table VIII, also include the time for which the cells were kept at the specific current density.

The total capacity delivered by cell 2 was 0.36 Ahr; the total available was 1.62 Ahr. Since only 22% of the available capacity was used in this test, these results are best considered as representing the initial capabilities of the cell, i.e., before substantial discharge-induced variations occur within the electrode structure.

Table VIII. Preliminary Performance Data of Li/Ni_3S_2 Cells in a 1M $LiClO_4$/THF

Cell 1			Cell 2		
Current Density, mA/cm^2	Time, min	Cell Voltage	Current Density, mA/cm^2	Time, min	Cell Voltage
0.5	15	1.37	0.5	15	1.38
1.0	15	1.35	1.0	17	1.37
2.0	20	1.33	2.0	15	1.32
4.0	15	1.23	4.0	15	1.23
5.0	-	-	5.0	70	1.16
3.0	-	-	6.0	42	1.14
10.0	12	<0.60			

Compared in Table IX are the overpotentials for the Li/Li and Li/Ni_3S_2 cells. Because of the uncertainty in the Ni_3S_2 half cell potential, the cell voltages at 0.5 mA/cm^2 were taken as the reference potentials. Although this detracts from the rigor of the discussion, it does provide a comparison of the initial cell polarizations due to the electrolyte-spacer (in the Li/Li cell) and due to the electrolyte-spacer plus pore structure (Li/Ni_3S_2 cell).

Table IX. Cell Overpotentials, mV

Current Density, mA/cm^2	Li/Li	Li/Ni_3S_2
1	0.00	10
2	5.0	60
4	-	150
5	27.0	220
10	63.0	>1000

The most obvious conclusion from these data is that most of the cell polarization is associated with the positive electrode rather than either the electrolyte, the separator, or the negative. The higher polarizations observed at the positive electrode can arise from several factors: (a) an inherently low exchange current for Ni_3S_2 reductions, (b) a reflection of poor mass transport within the electrode pore structure, and (c) passivation of internal and/or external surface area with a film

of Li_2S. Obviously, items (b) and (c) are highly dependent on the electrode structure. These interrelationships between structure, electrolyte, and performance are considered in detail in Part C, which follows. Measurement of the exchange current requires an electrode of well-defined surface area and composition. Although electrochemical measurements were not made, pure Ni_3S_2 material (in ingot form) was prepared via direct fusion of the elements. This proportion and a description of the material is given in Appendix 1.

2. Electrolyte Purification

During these early experiments, occasional anomalies in the discharge behavior of the Ni_3S_2 appeared. These deviations, which were associated with specific batches of THF, were of the form shown in Fig. 1. As can be seen, oscillations in cell voltage (e.g., ±0.2V at 0.3 cycles/min) appeared during an otherwise normal discharge. These episodes (whose initiation time varied from cell to cell) were followed by a gradual voltage decay to 0V.

In order to clarify this failure mechanism, two cells were discharged at 2 mA/cm^2. One cell oscillated and delivered 39% of capacity to 0V. The second cell, which did not oscillate, delivered 44% of capacity. The positive electrodes were then removed and assembled into new cells (new separator and lithium electrodes). An additional 40% capacity (to 0V) was achieved with each cell. This fact strongly suggests that the failure mode was not associated with the Ni_3S_2 positive.

In order to test the negative, a cell was operated until the oscillations and voltage falloff occurred. A coulombic utilization of 40% was obtained to a 1V endpoint. The separator and electrolyte were replaced and the cell reassembled. A current density of 3 mA/cm^2 could not be sustained. When the lithium electrode was replaced, however, an additional 20% capacity was achieved at 3 mA/cm^2.

That lithium can react chemically with the THF-$LiClO_4$ solution used in these cells was confirmed by the following experiment. A three-compartment cell was constructed with a lithium foil anode (1 cm^2) as the test electrode, a lithium counter, and a lithium reference electrode. A Luggin capillary was placed at the rear of the anode; the electrolyte was untreated THF-$LiClO_4$. Anode polarization as a function of current density is shown in Table X.

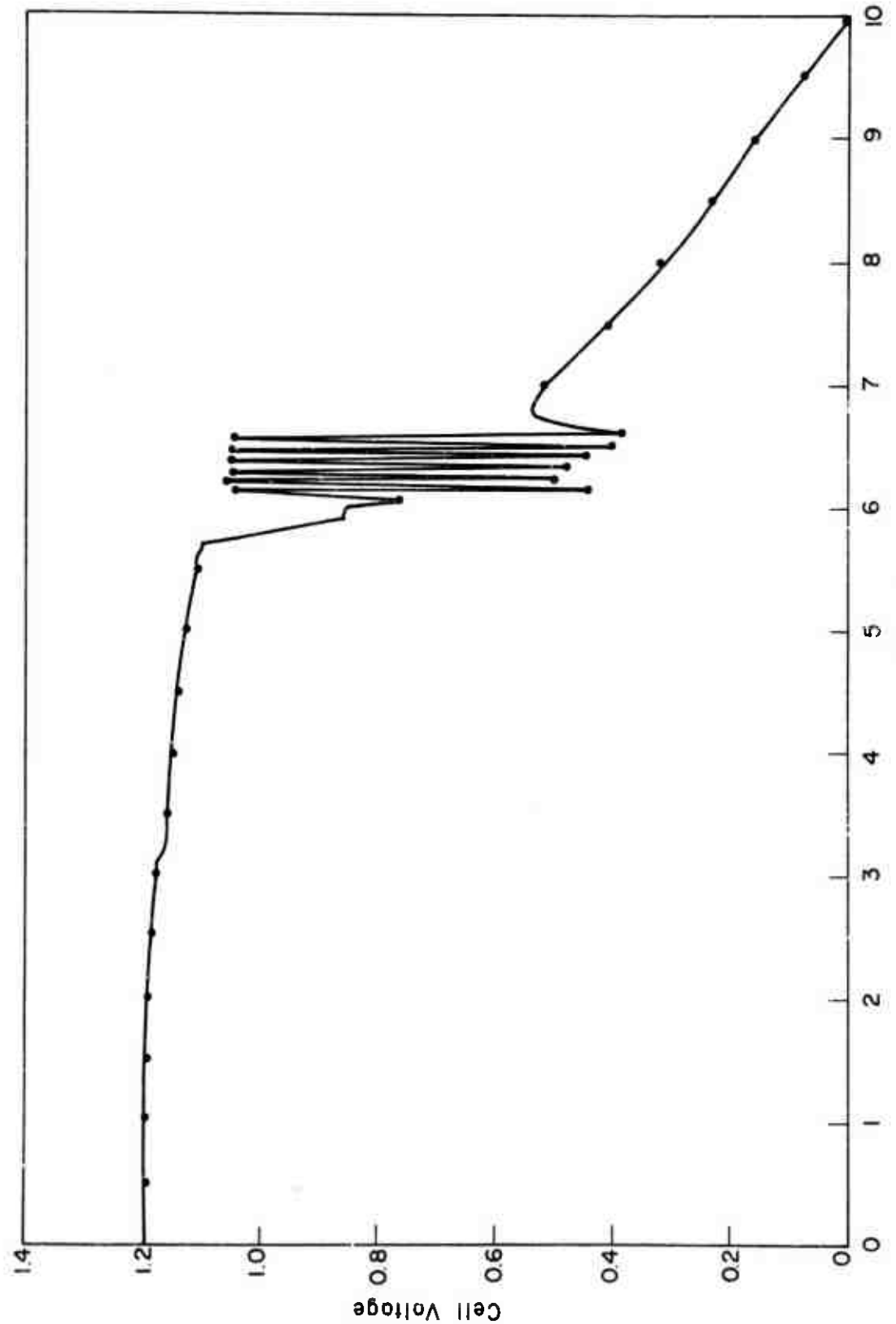

Fig. 1. Discharge curve at 3 mA/cm^2 for a Li/Ni_3S_2 cell illustrating anomalous voltage oscillations

Table X. Lithium Anode Polarization
(Untreated THF-$LiClO_4$)

Current Density, mA/cm^2	Cumulative Time, min	Potential Change, mV
0.2	125	2.5
0.5	145	7
1	160	12
2	175	16
3	190	19
3	240	21
3	300	23
3	480	25
3	600	29
3	720	36
3	840	43
3	960	51
3	1080	84
3	1200*	1000

* Coulombic Utilization 27%

After an initial 180 min, a black film was observed to form on the edges of the lithium anode. By 240 min, the entire face of the lithium anode towards the counter-electrode had turned black. At this stage, only a small change in overvoltage was noted, indicating, most likely, a porous film. As the discharge continued, high polarizations were reached; the bottom of the electrode was very brittle and broke off on agitating the solution.

Since lithium reacts with the electrolyte, pretreatment with lithium dispersion should remove the problem. A series of cells were run which differed in a number of aspects, including pretreatment of the electrolyte. The end-of-discharge performances are displayed in Table XI according to this variable.

Table XI. Failure Mode Frequency Versus Electrolyte Treatment

Item	Total No. of Cells	Failure Mode		
		Oscillation	Abrupt*	Gradual
Dispersion treated	10	1	6	3
Untreated	17	9	6	2

* Cell failure by direct shorting due to migration of Ni_3S_2 particles through the separates.

Thus, it seems that: (1) the oscillations are caused by an interaction of lithium and an electrolyte impurity, and (2) this problem can be cured by treatment of the electrolyte with lithium dispersion. This impurity appeared to be present in electrolyte prepared from each cut taken in the particular distillation run. This is shown in Table XII.

Table XII. Failure Mode Versus Distillation Cut - Untreated

Cut	Total No. of Cells	Oscillations	"Abrupt"
3	10	4	3
4	6	3	2
5	1	1	-

In view of the simple treatment procedure, further investigation of this impurity problem was not performed. It remains to be established, for example, whether the contaminant is present in the salt or the solvent or whether the contaminant is generated on standing.

C. Positive Electrode Optimization

Definitive optimization of an electrode structure requires a relatively extensive experimental program. The interrelationships between the structural variable (e.g., initial particle size, compaction pressure, and/or binders) and the microscopic and macroscopic structure (e.g., porosity, surface area, and strength) are sufficiently complex that for practical purposes an empirical approach to electrode optimization becomes mandatory. Thus, the following experimental program, designed to explore the effects of changes in positive electrode construction variables on both coulombic and voltage efficiency, was carried out in a configuration approximating a working cell. The objective of these experiments was to determine to what extent the relatively high polarization observed for Ni_3S_2 electrodes in Part B was associated with the structure of the positive electrode.

The specific method of constructing the test cells was as follows: 3.3 g Ni_3S_2-Al (5, 10, or 20%) was pressed on an aluminum grid at 4 to 15 tons to form a circular electrode with a diameter of 1.75 in. Folded around this electrode was a 4-in. × 2-in. piece of lithium ribbon. The electrodes were separated by a layer of non-woven Pellon polypropylene fabric. The cell assembly was then enclosed in a thin polyethylene bag with 1 M $LiClO_4$/THF. In order to simulate the electrode environment in a multiplate stack, the cell package was inserted between two metal plates which were hand tightened to maintain an evenly distributed pressure on the cell electrodes.

As a result of the high volatility of THF (b.p. 65°C), it became necessary to seal the bag cell to prevent drying out of the electrodes. Thus the top of the polypropylene bag was heat sealed over the grid tabs. An Al grid was used as a tab for the Ni_3S_2 electrode and a Ni grid was used as a tab for the Li. This partially effective method was later improved by using self-sealing ("zip-loc") bags.

To further reduce drying out of the cell by THF evaporation, the entire cell assembly was put into an enclosed metal cyclinder containing an open beaker of THF. This caused the atmosphere around the cell to be saturated with THF and, as a result, the loss rate of the THF from the bag cell was significantly reduced.

In the presence of THF, a greasy film formed between the Ni grid tab and the Li metal folded around it. This resulted in a loss of contact with the cell. A Cu grid rinsed in acetone was tried but also was unsuccessful. The same results occurred when an alligator clip (either Cu or Cd plated Stainless Steel) was attached to a Li tab extending from the electrode outside the cell (presumably because of the THF saturated atmosphere in the cylinder). This problem was finally solved by: (1) the use of a long Li tab extending from the cell to outside of the cylinder, and/or (2) the use of a Ni grid rinsed in trichloroethylene.

The next operational problem encountered was a brownish precipitate formed after the electrolyte was added to the cell. Pressure caused the cell performance to decay rapidly. The deposit was found to have been caused by a reaction between Li and $LiClO_4$ - THF solution dried with molecular sieves. This drying procedure was therefore replaced by the electrochemical water-reduction process developed previously for use with cyclic esters.

1. Preliminary results

Some test data were acquired while the above test procedure was being evolved. These data are discussed below. The variables under concern were: (1) the pressure applied to the disk, (2) the quantity of aluminum fiber, and (3) the quantity of active material and hence the thickness of the electrode. Emphasis was placed on the first two.

Shown in Fig. 2 is a potential-time curve for a cell operated under the following conditions: current density 3 mA/cm^2, 3.6 g of Ni_3S_2 plus aluminum (18%), and 10 tons formation pressure. In all tests, the electrolyte was standardized as 1 M $LiClO_4$ in THF. Before recording the data in Fig. 2 the cell was discharged at 0.5 and 4.5 mA/cm^2, each for 2 hr, to remove residual water. The difference in plateau voltage for this cell and those noted in Table VIII is due to the longer time the cell of Fig. 2 was first operated at 4.5 mA/cm^2.

This form of discharge curve is reasonably typical, including the rapid falloff at the termination of the discharge. It is apparent from the shape of this discharge curve that the effective coulombic efficiency could be sensitive to fluctuations in operating potential, e.g., small spurious increases in internal resistance. For example, at 1 V, a variation of ±30 mV would alter the use efficiency by ±3%; a variation of ±100 mV would alter the efficiency by ±25%.

The test of cell performance was taken as the percent net utilization to a 1.0 V

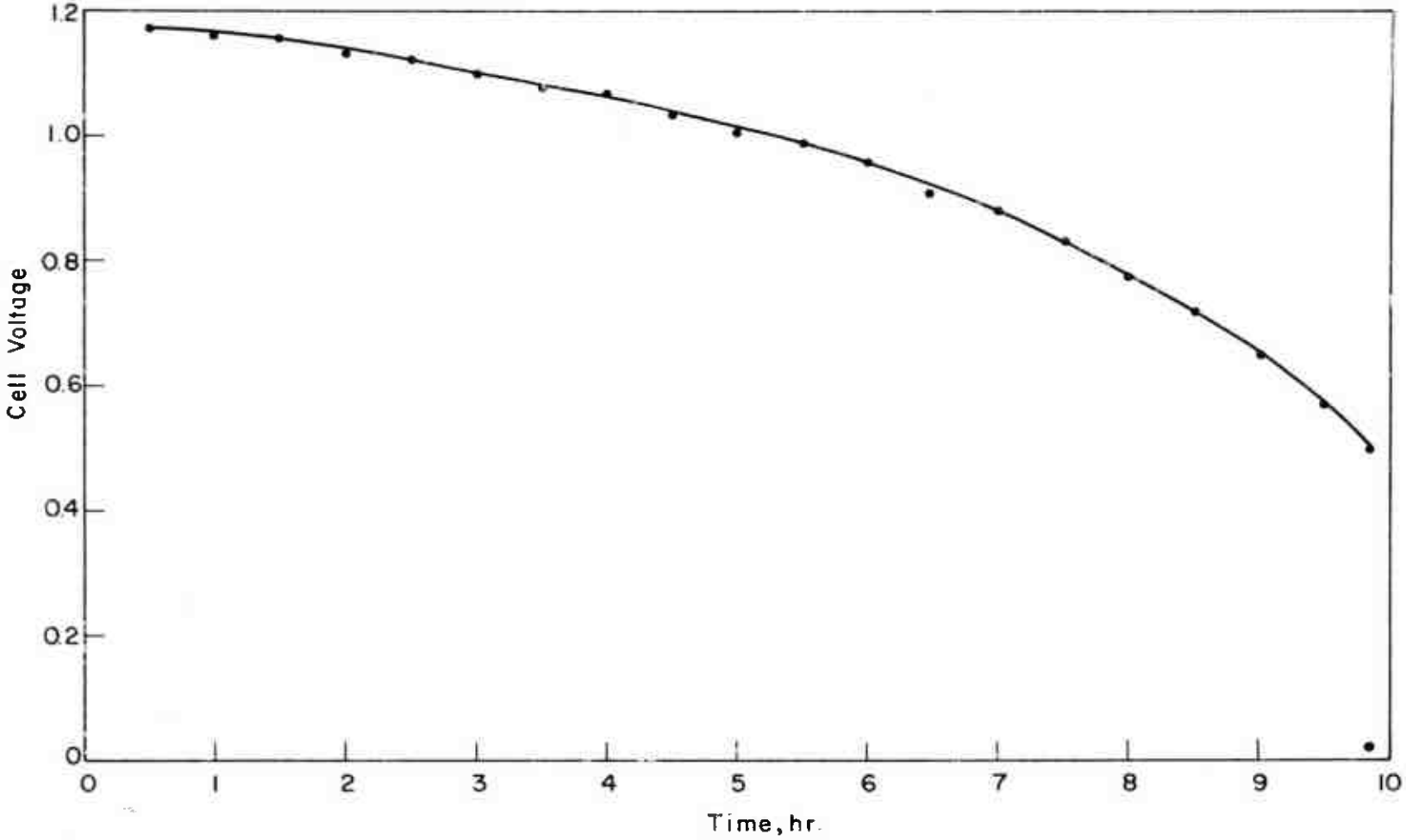

Fig. 2. Typical potential time curve at 3 mA/cm^2 for the cell: Li/1M $LiClO_4$, THF/Ni_3S_2, Al

cutoff at a fixed current density. Much of this work was carried out at 3 mA/cm^2 and some at 4.5 mA/cm^2.

In Table XIII is summarized the coulombic efficiencies as a function of positive electrode compaction pressure.

Table XIII. Effect of Compaction Pressure on Performance

Total Pressure (tons)	% Utilization, at 3 mA/cm^2 (the 10-hr rate)
4	90
6	68
8	65
10 (Fig. 1)	50

Reducing the aluminum fiber content from 20% to 5% reduced the coulombic efficiency from 50% to 40% at 10 tons and from 65% to 50% at 8 tons. Increasing the current density to 4.5 mA/cm^2 at 10 tons (20% Al) dropped the use efficiency from 50% to 40%. These effects are all in the direction anticipated.

For the purpose of comparison, identical experiments were carried out with butyrolactone as the electrolyte solvent. The cell potential dropped below 1 V within 20 min at a current density of 2.0 mA/cm^2. An electrode pressed at 10 tons gave 15% utilization at 1.5 mA/cm^2; an electrode pressed at 8 tons gave 41% utilization at the same current density. It is thus apparent that the THF/$LiClO_4$ electrolyte represents a substantial improvement over the electrolyte solution used in earlier work. Although the rate capabilities of the Ni_3S_2 do not appear to be limited by the mass transport capabilities of the solvent (as was apparently the case for PC and BC solutions), cell polarizations are still relatively high. Further optimization of rate capability was attempted by altering the electrode's pore structure in order to: (a) provide as much surface as possible, and (b) prevent pore blockage and occlusion of electrode surface by Li_2S deposited during discharge.

2. Structural modifications

The objective in this experimental area was to increase both electrode surface area and porosity so as to maximize the effective Ni_3S_2 surface. These desirable features can be generated by reducing the compaction pressure used to form the electrode. Unfortunately, this approach has its limits since the physical coherence of the electrode drops sharply as its gross porosity falls below 50%.

The classical approach to obtaining high porosities simultaneously with reasonable physical integrity is the addition of a bonding agent to the electrode mix. For use with the cell system under consideration, the binder must be free of water and insoluble in the electrolyte. Teflon dispersion was studied, using the preparation techniques developed previously for fuel cell electrodes.

A 0.75-in. × 0.75-in. × 0.005-in. aluminum grid was coated on both sides with a mix of 0.900 g Ni_3S_2 + 20% aluminum fiber plus 0.39 g Teflon. This 30% (by weight) Teflon-bonded electrode was then sintered under nitrogen at 280° for 1 hr. To increase adherence of the active material, the electrode was then compressed by rolling with a glass cylinder; pressing at 1,000 lb was also effective, while pressing at 5,000 lb resulted in an inoperative electrode. A rolled electrode was then discharged at 2.5 mA/cm^2. The utilization was 58% to a 1 V cutoff; a plateau was observed at 1.22 V.

Loadings were then varied from 10 to 30% Teflon; sintering times were varied from 20 min to 2 hr; electrodes were tested as 2.9 cm^2 disks. In Table XIV and Fig. 3 are shown the dependence of cell voltage on current density for cells prepared with 30% Teflon but with variable sintering times; each point was taken after at least 30 min at the specified voltages.

Table XIV. Current Density – Potential Dependence (30% Teflon-Bonded Electrodes)

	Cell Voltages							
Cell Number	1	2	3	4	5	6	7	8
Sintering Time	20 min	30 min	1 hr	2 hr	30 min	2 hr	2 hr	Zero Teflon
Current Density mA/cm^2								
0.4	1.68	1.60	1.64	1.62	1.65	1.60	-	-
1	1.52	1.40	1.46	1.48	1.46	1.42	1.42	1.44
2	1.34	1.22	1.30	1.28	1.22	1.26	1.28	1.10
3	-	-	-	-	-	-	1.23	0.9
4	1.12	1.16	1.20	1.10	0.95	1.18	1.18	-
6	0.86	1.0	<0.8	-	unst.	-	-	-

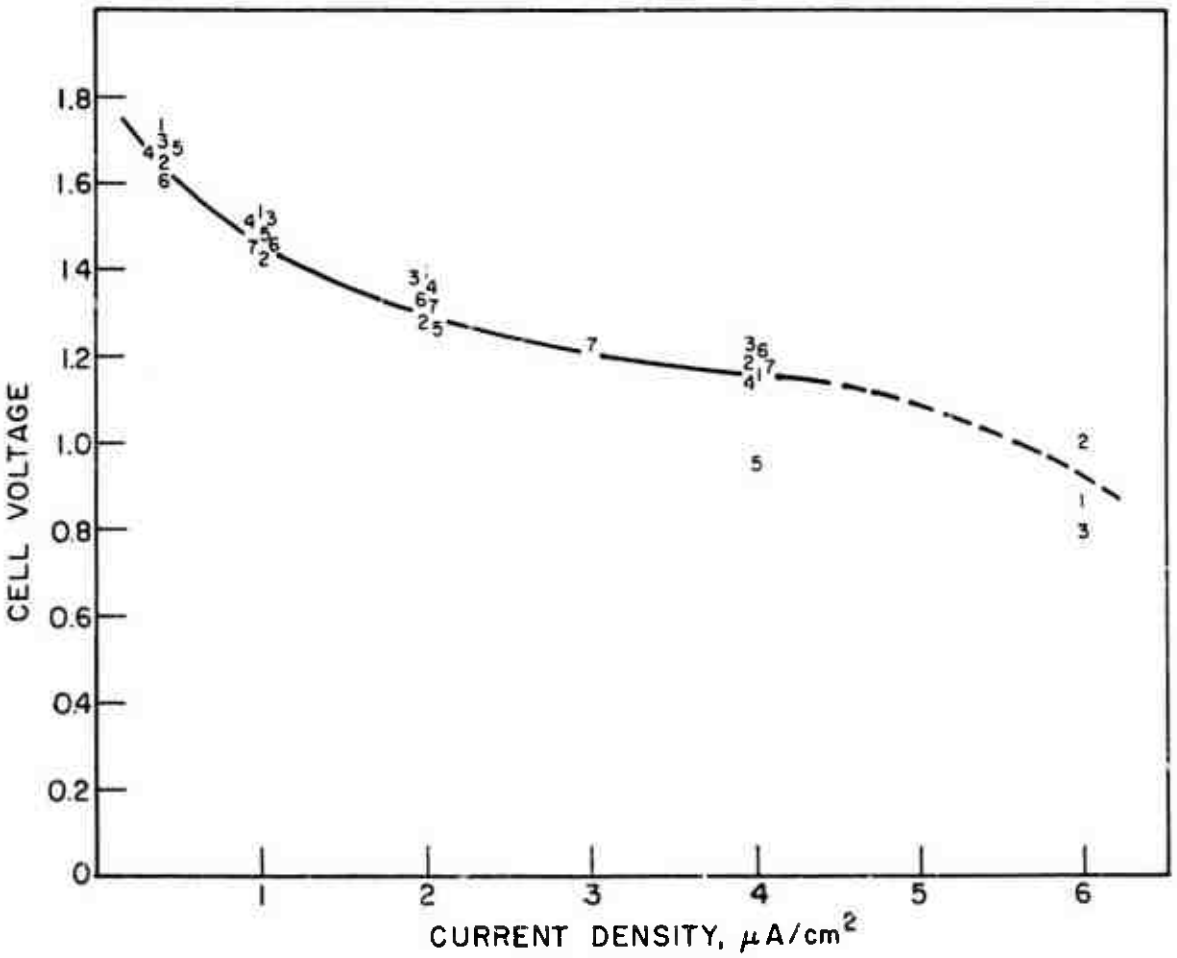

Fig. 3. Repetitive current-potential curve for Li/THF/Ni_3S_2 cells

Best results were obtained with electrode preparation #1 (30% Teflon, sintered for 30 min). This electrode exhibited significantly better performance (particularly at current densities above 1 mA/cm^2) than those observed for unteflonated electrodes. In the case of the teflonated positives, stable discharges were obtained at current densities corresponding to a 10-hr discharge rate.

In Table XV are shown the percent utilization of the positive plate for a number of these cells subjected to extended discharge. The following conclusions can be made: (1) significant utilizations of active material are possible at 2.5 and 4 mA/cm^2, and (2) the active material is only approximately described as Ni_3S_2.

Table XV. Positive Plate Utilization

Current Density, mA/cm^2	% Utilization, to 1 V	% Utilization, to 0 V
2.5	48	58
4	37	109
4	0	95
4	41	69

Having demonstrated the general approach, a few experiments were run in an attempt to reduce the Teflon content. In Table XVI are shown the current potential dependence for one cell containing a positive electrode with 10% Teflon and sintered for 2 hr. These voltages are somewhat higher than shown in Table XIV for 30% Teflon electrodes, which would be consistent with a lower internal resistance. Obviously, however, one run is insufficient to substantiate such a conclusion with any degree of confidence.

Since satisfactory performance was obtained in the short time, this cell was discharged at 4 mA/cm^2 to completion. A utilization of 54% was obtained to a 1.0 V endpoint; 90% was obtained to 0 V. Thus it would appear that lower Teflon contents are indeed feasible.

An interesting feature of the Teflon-bonded positives was their ability to prevent Ni_3S_2 migration through the cell separator. This failure mode was a frequent occurrence in cells discharged at high current densities in THF-based electrolytes (See Table XII). Cell failure by direct shorting had not been observed in the past with either propylene carbonate or butyrolactone (even when these last electrolytes were used in cells discharged at high rates).

Table XVI. Performance of Teflon-Bonded Positive

Current Density, mA/cm^2	Voltage, V		
	10% Teflon	20% Teflon	20% Teflon
0.4	1.74	1.62	1.66
1	1.56	1.48	1.54
2	1.42	1.20	1.38
4	1.22	0.40	1.14

For example, a cell using BL as the solvent yielded 26% theoretical capacity at 2 mA/cm^2. The cell's voltage decay was gradual and the cell exhibited no anomalous behavior. Another cell, using THF discharged under the same conditions, failed abruptly after 44% utilization. Obviously, these results are not directly comparable since the abrupt failure could be associated with the deeper depth of discharge obtained from the THF cell. However, the depth of discharge does not appear to be of overriding importance since cells containing THF, discharged at low (e.g., 0.5 mA/cm^2) current densities to approximately the same depth of discharge, did not exhibit Ni_3S_2 migration and direct shorting.

Why should Ni_3S_2 penetrate the separator? Crystalline lithium sulfide has a density of 1.66 g/cc, crystalline nickel sulfide has a density of 5.82 g/cc, and nickel has a density of 8.90 g/cc. Thus a plate of 1 g of Ni_3S_2 discharging via:

$$Ni_3S_2 + 4\,Li^+ + 4\,e^- \rightarrow 2\,Li_2S + 3\,Ni$$

would expand in volume from 0.17 to 0.31 cc* (assuming crystalline materials). The higher the current density the faster would be the rate of expansion. It would be expected that the particle size and volume of the precipitated Li_2S could depend on electrolyte. Thus expansion could be a problem in one system and not another. Presumably the increased electrode porosity present in the teflonated electrodes compensates for the apparently larger volume of Li_2S which is produced in the THF at high discharge rates.

* As far as total cell volume is concerned; there will be some compensation by a decrease in volume of the lithium electrode, in the example given, this discharge would result in a volume decrease of 0.22 cc. The net change then is a percent increase of:

$$\frac{0.31 - 0.22}{0.17 + 0.22} \times 10^2 = \frac{9}{39} \times 10^2 = 23\%.$$

IV. PROPERTIES OF AIR-OXIDIZED Ni_3S_2

Oxidation of Ni_3S_2 was first investigated by heating a complete Ni_3S_2 electrode in air at 325°C for 15 min. The circular, flat electrode was 0.035 in. thick and had a current area of 30 cm^2 (1.75 in. in dia). Fig. 4 illustrates two typical room-temperature discharges carried out in a polyethylene bag cell. At a drain of 0.5 mA/cm^2, the oxidized electrode exhibits two clearly defined plateaus at 1.67 V and 1.40 V. The non-oxidized electrode (pure Ni_3S_2) exhibits only a single plateau at 1.40 V. The high voltage plateau represents about 40% of the useful capacity of the battery.

As a quick check on the stability of the high voltage material, similar oxidized electrodes were discharged at different rates (0.5 mA/cm^2 and 0.25 mA/cm^2). The ampere-hour capacity on the high voltage plateau was the same in both cases, indicating that the oxidized material is substantially insoluble in the cell electrolytes.

As a first attempt to increase the high voltage capacity, a Ni_3S_2 electrode was heated for 4 days at 325°C. Its high voltage plateau was identical to the electrode in Fig. 1, which had been heated for only 15 min. The conclusion is that in air, at 325°C, the reaction is rapid and probably involves only the surface of the Ni_3S_2 particles.

The effect of oxidation temperatures up to 500°C is shown in Fig. 5. Discharges at 0.77 mA/cm^2 for oxidation temperatures of 400°C and 500°C are shown. A similar discharge of a non-oxidized electrode is given for comparison. The results at 400°C are similar in form to those at 325°C (Fig. 4). Approximately 40% (0.54 Ahr) of total theoretical capacity is obtained on the high voltage plateau. Further increases in the oxidation temperature resulted in a marked deterioration in electrode performance. These electrodes (e.g., 500°C) were brittle and easily broken. Undoubtedly, this change in gross physical preperties was accompanied by a similar loss in electrode porosity.

In order to avoid interactions between the oxidation step and the electrode structure, an attempt was made to oxidize the Ni_3S_2 powder prior to fabricating the electrodes. For these runs, the Ni_3S_2 powder was heated on a pyrex watch glass and

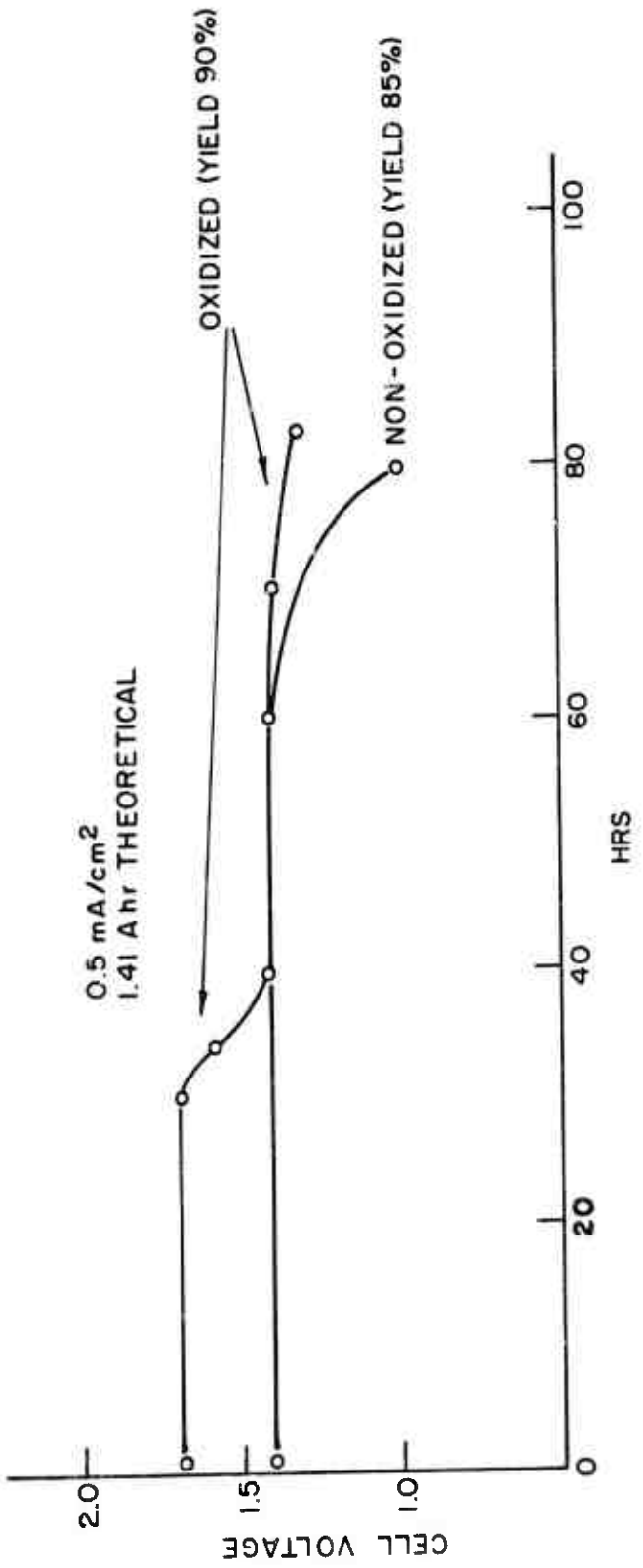

Fig. 4. Discharge performance of oxidized and non-oxidized nickel sulfide electrodes at low rates in PC

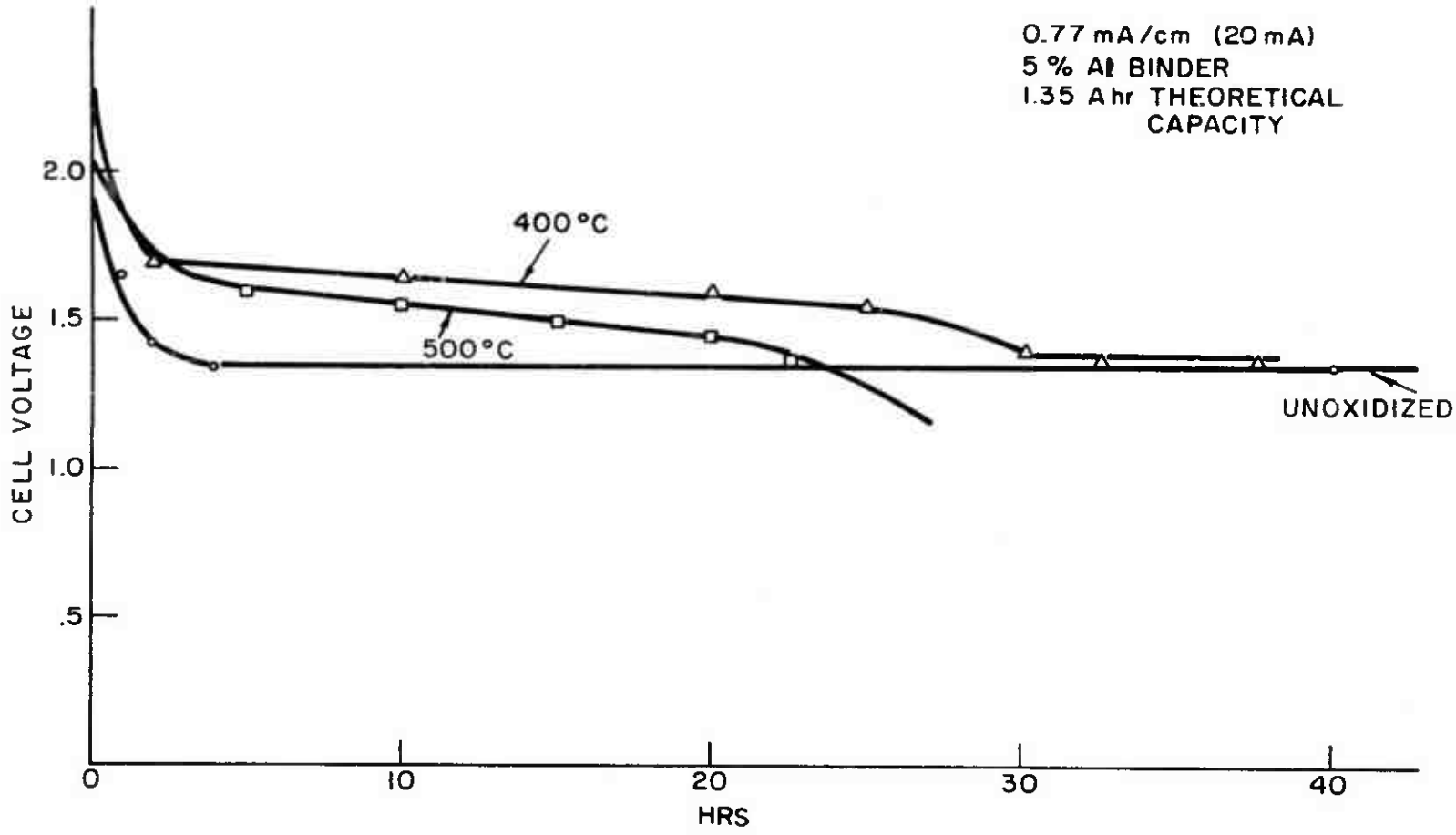

Fig. 5. Effect of temperature on the air oxidation of Ni_3S_2 electrodes

then fabricated into electrodes using the standard pressure of 13,600 lb. It was found, however, that electrodes as thin as 0.030 in. could not be prepared due to the low cohesiveness of the oxidized particles. Thus, electrodes prepared by this method were formed from ≈6 g Ni_3S_2 instead of the 3.0 g Ni_3S_2 previously used.

The results obtained by heating the Ni_3S_2 powder at 400°C and 450°C are shown in Fig. 6. Note that the current density has been reduced by a factor of 2 to 0.4 mA/cm^2 as a result of the high polarizations observed with these electrodes. The electrode containing powder heated at 400°C exhibits evidence of the same high voltage plateau observed in previous work with heated electrodes. The overall performance is quite poor, however. The results from the run at 450°C, although even poorer from an electrochemical-yield standpoint, are instructive. Although no significant capacity was obtained above 1 V versus lithium, a stable plateau exists at approximately 0.5 V versus lithium.

The overall results obtained from these two runs are consistent with the creation of an insulating powder which would be expected to require more careful attention to electrode structure before exhibiting respectable coulombic efficiency. The existence of a stable plateau at ≈0.5 V was subsequently shown (see Part V) to indicate a degeneration of the Ni_3S_2 material into NiO. Thus, at this stage, the nature of the high voltage material had not been clarified.

X-ray diffraction patterns were therefore obtained from samples of Ni_3S_2 powder, both in the "unoxidized" state and after being heated at 325°C for one hour. The unheated material was found to be predominantly Ni_3S_2 with significant quantities of Ni_7S_6. The treated material was determined to be a mixture of $NiS_{1.09}$ and Ni_7S_6. Thus, oxidation of Ni_3S_2 appears to result in a shift towards the sulfur-rich nickel sulfides. Such materials are known to have higher discharge voltages and to yield higher energy densities than simple Ni_3S_2. For example, the cell reaction:

$$NiS + 2\,Li \rightarrow Ni + Li_2S \qquad (6)$$

has a thermodynamic potential of 2.2 V and a theoretical energy density of 514 Whr/lb, as compared with an observed potential of 1.4 V and a theoretical energy density of 254 Whr/lb for Ni_3S_2.

The presence of some Ni_7S_6 in untreated Ni_3S_2 is to be expected from the ambient temperature oxidation of Ni_3S_2. Freshly prepared Ni_3S_2 shows no evidence of Ni_7S_6. Long term storage of Ni_3S_2 in the laboratory results in an easily observable darkening of the surface of the high surface area particles.

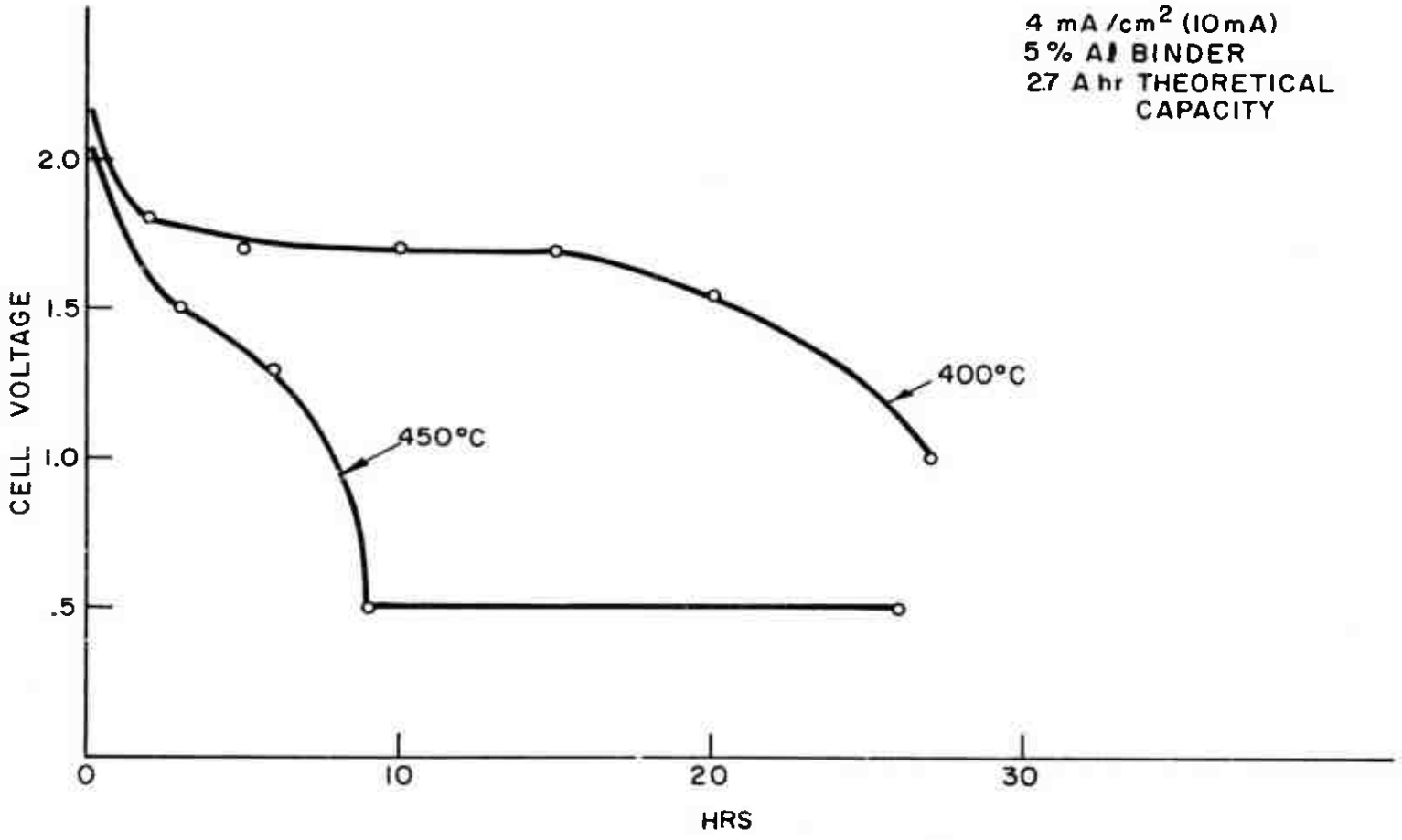

Fig. 6. Performance of oxidized Ni_3S_2 electrodes (oxidation prior to fabrication)

In an attempt to confirm the X-ray analysis, an electrode comprising commercially available NiS and 20% Al fiber was prepared. The electrode contained 6 g of NiS. When discharged at 0.4 mA/cm^2, a single sloping plateau of low coulombic capacity from 2.4 to 2.1 V versus lithium was observed. Only 100 mA/hr were obtained from this electrode. However, discharge of an oxidized electrode composed of equal amounts of commercial NiS and Ni_3S_2 did not exhibit a plateau above 2 V. On the contrary, electrode performance was poorer than that observed from oxidized electrodes containing no NiS.

Thus, experimental confirmation of the X-ray analysis could not be ohtained. Whether this failure arose from the use of NiS instead of $NiS_{1.09}$ cannot be stated with certainty, since the experimental results are confounded by unavoidable alternations to the microstructure of the test electrodes. This difficulty is clearly evident in the comparison of the discharge of commercial NiS (a significant plateau above 2 V) and the 50/50 mixture of NiS and Ni_3S_2 (no plateau above 2 V). Better defined starting materials will be required to elucidate the electrochemical behavior of the alternative nickel sulfides.

V. ALTERNATIVE POSITIVE MATERIALS

Although, as described in Section III, the high rate and, presumably, the low temperature performance of the Ni_3S_2 system are considerably improved through the use of a less viscous THF electrolyte, it is clear that the principal performance limitation lies in the basic discharge behavior of Ni_3S_2 in the specific electrolyte chosen. Despite the fact that there are obviously some rate limitations inherent in the mass transport properties of the electrolyte solvent, the best rates obtained with improved Ni_3S_2 electrode structures are still lower than those obtainable with alternative positive materials.

The relatively limited rate capability of Ni_3S_2 is currently presumed to be determined by its extremely low solubility in aprotic solvents. Since it is precisely this latter property which contributes to the Li/Ni_3S_2 system's outstanding shelf life, it will be necessary to accept some deterioration in standby performance if high rate performance is to be improved. The extent to which cell performance is limited by the formation of Li_2S on the Ni_3S_2 has not been investigated in detail. Characterization of the passivating film and the use of approaches based on the creation of a porous coating should be considered in further work.

Thus, the work described in this section represents a shift in emphasis from electrolyte studies to an investigation of electrode materials. Three classes of inorganic positives were screened for use as cathodes in high rate non-aqueous systems: (1) metallic oxides, (2) metallic carbonates, and (3) metallic cyanides. The compounds were first evaluated on the basis of thermodynamic feasibility (e.g., cell voltage and equivalent weight). This preliminary work was followed by a rapid screening program using small, non-optimized electrodes in excess electrolyte ($PC/LiClO_4$). Some of the more promising materials were also evaluated in full cell tests to check on negative/positive compatability and solubility characteristics.

A. Half-Cell Screening

The data obtained for all tested materials is contained in Table XVII. Discharge curves for the oxides, carbonates, and cyanides are presented in Figs. 7, 8, and 9, respectively. Electrochemical performance was determined in a standard three compartment cell using a lithium counter-electrode and a lithium reference electrode. The positive electrode materials (reagent grade and mixed with ~20% Al binder) were pressed on a nickel screen of approximately 1 cm^2 area. In the case of hydrated materials, the reagents were dried under inert gas. The electrolyte in all cases was 1 M $LiClO_4$ in PC. All discharges were at 1 mA constant current.

1. Metallic oxides

For the materials tested, energy densities ranged from 297 Whr/lb for CdO to 711 Whr/lb for a 4 electron reduction of MnO_2. Only ZnO, CuO, and NiO exhibited significant capacity when discharged in PC/$LiClO_4$. Coulombic utilizations obtained from NiO and ZnO were quite high, although in both cases the electrode potential was much lower than that predicted by a reaction of the type:

$$MO + 2Li \rightarrow Li_2O + M \qquad (7)$$

Reducing the current drain did not significantly increase the discharge potential. In the case of ZnO, reducing the discharge rate by a factor of 20 to 0.05 mA increased the potential by only 50 mV. In spite of the lack of correspondence to thermodynamic value, the reduction of the ZnO to metallic zinc was confirmed visually.

In order to ascertain the effect of electrode structure on the discharge of NiO, a brief full cell testing program was performed. High surface area NiO was prepared by the thermal decomposition (≈ 350°C) of hydrated $NiNO_3$. Lithium doping (to improve the conductivity) of the NiO was accomplished by dissolving $NiNO_3$ in water and adding the required amount of $LiNO_3$ solution. The excess water was evaporated to form a stiff paste which was then transferred to a tube furnace for decomposition under inert gas.

The results obtained from these larger NiO electrodes were disappointing Although stable plateaus were again found to exist at 0.5 to 0.6 V versus lithium these plateaus were fairly insensitive to electrode modifications which would be expected to improve conductivity. Polarization was high even at the lowest drain rates. Thus, it was concluded that discharge of NiO in $LiClO_4$/PC electrolytes is limited by the discharge behavior of electrode material rather than by structural

Table XVII. Properties of Materials Screened for Suitability as Cathodes in Aprotic Organic Electrolyte Cells

Material	Electrode Weight (mg)	Theoretical Capacity (Ahr/g)	Percent Utilization	Thermodynamic Potential vs. Li (V)	Theoretical Energy Density* (Whr/lb)	Observed Plateau (V at 1mA/cm^2)
Metal Oxides (Fig. 4)						
CdO	75.6	0.42	3%	1.73	297	None
ZnO	60	0.66	>90%	1.26	322	0.6
CuO	32	0.67	50%	2.22	575	1.27
MnO_2 (Teflon Binder)	65	1.23	0%	1.68	711	None
NiO	70	0.72	75%	1.76	490	0.55
Metal Carbonates (Fig. 5)						
$NiCO_3$	106	0.45	50%	2.67	488	Sloping From 1.0
$CoCO_3$	41.8	0.45	50%	2.5	457	Sloping From 0.9
$CuCo_3$ [$\cdot Cu(OH)_2$]	53.3	0.48	45%	~3.16	~612	Sloping From 1.6
$MnCO_3$	95	0.47	0%	0.86	163	None
Metal Cyanides (Fig. 6)						
AgCN	144	0.2	55%	~2.6	~224	1.8
CuCN	104	0.30	60%	~2.1	~265	1.4
$Cd(CN)_2$	72	0.33	0%	~1.8	~248	None
$Co(CN)_2$	65	0.49	0%	–	–	None
$Hg(CN)_2$	228	0.21	5%	~2.3	~208	Sloping from 1.8
$Ni(CN)_2$	71	0.48	0%	~1.6	~310	None

* Includes the required lithium metal

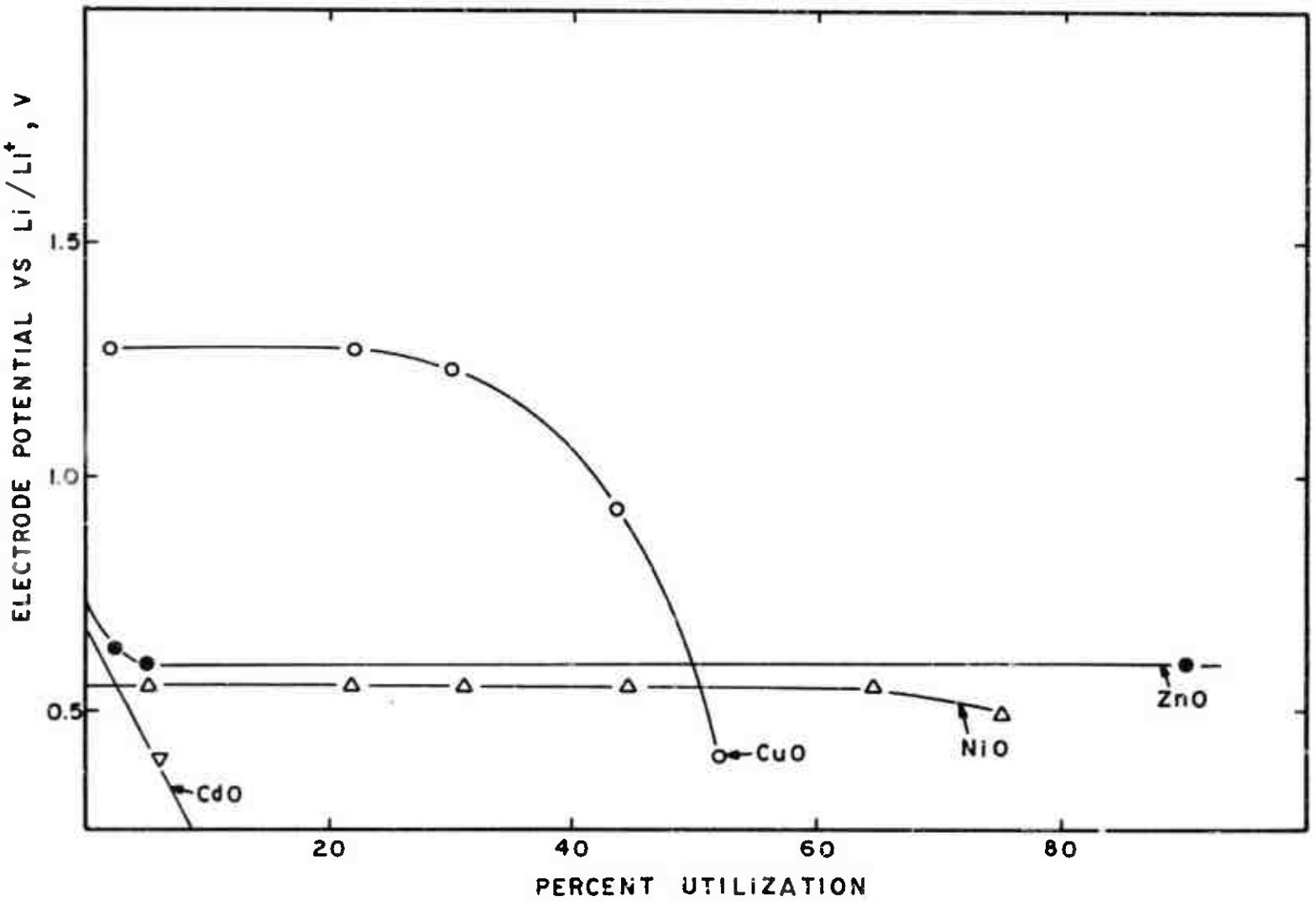

Fig. 7. Half-cell discharges of metal oxide electrodes in PC/$LiClO_4$ at 1 mA/cm^2

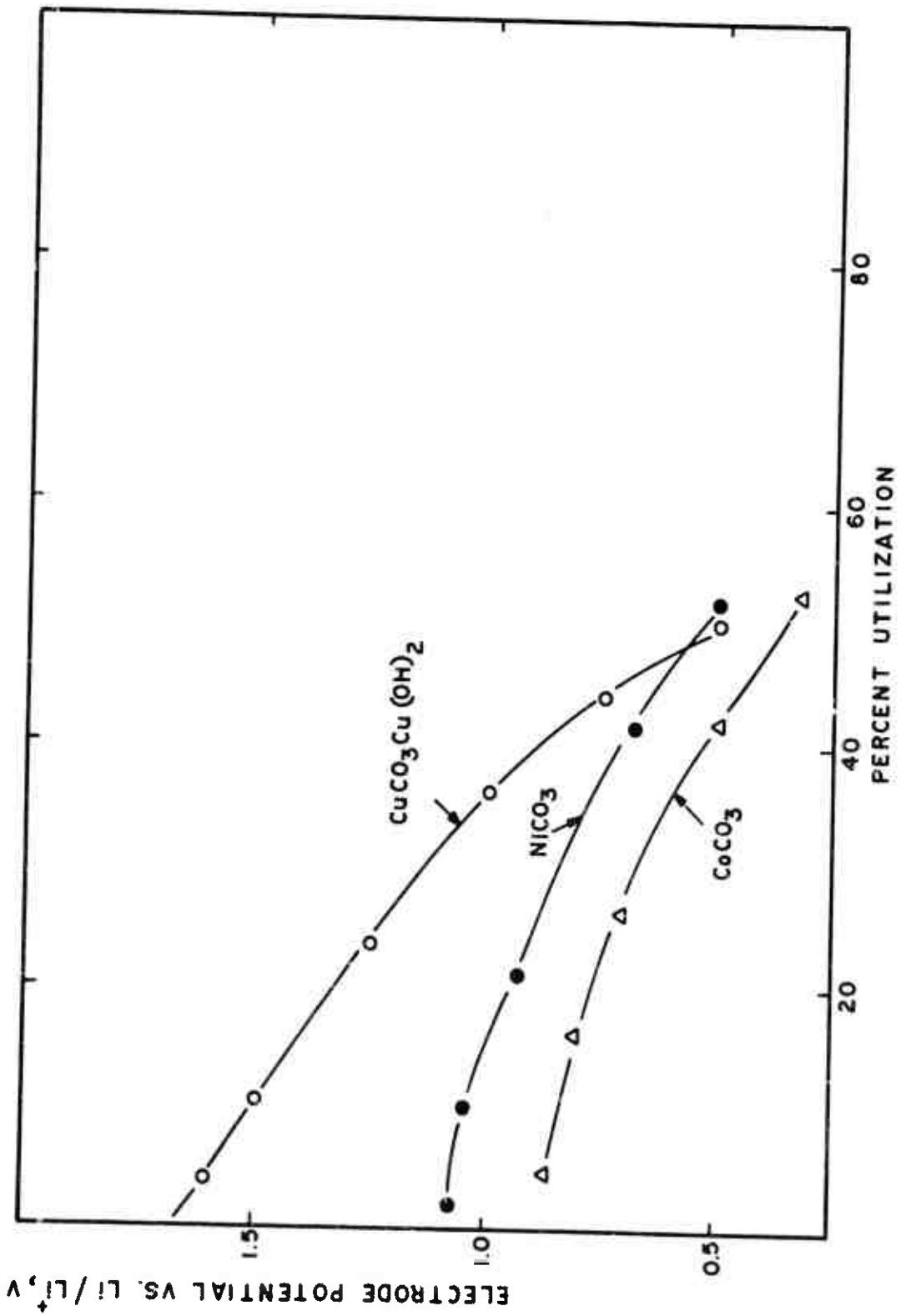

Fig. 8. Half-cell discharges of metal carbonate electrodes in PC/$LiClO_4$ at 1 mA/cm^2

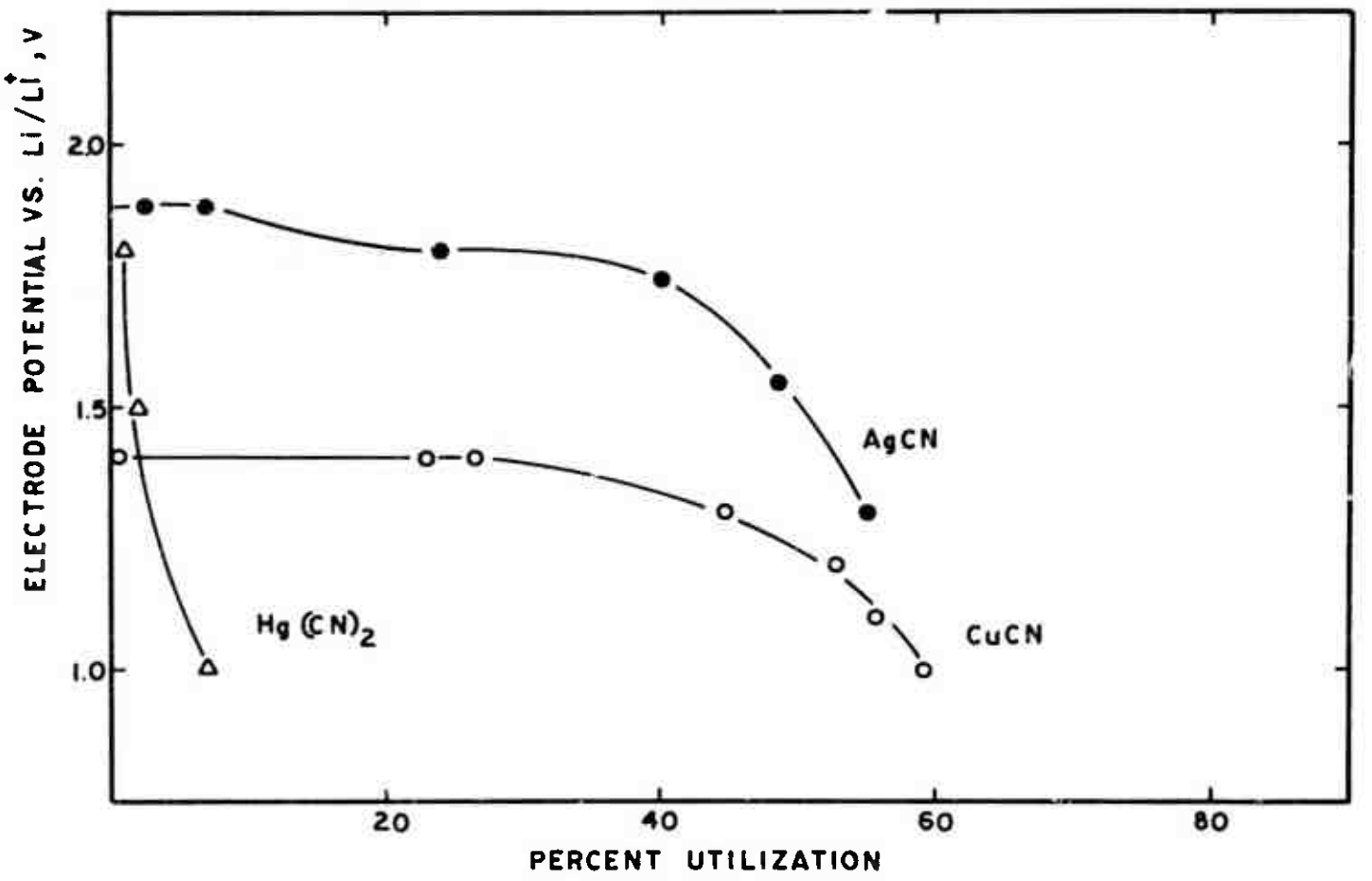

Fig. 9. Half-cell discharges of metal cyanide electrodes in PC/$LiClO_4$ at 1 mA/cm^2

problems arising from the fabrication of electrodes from an insulating material.

Table XVIII summarizes some of the results obtained. The principal variables were compaction pressure (porosity), quantity of aluminum binder, and quantity of lithium dopant. Plateau voltages were taken as a measure of performance. Coulombic capacities were not determined in view of the high polarization. All electrodes contained 6 g NiO and were discharged in polyethylene bag cells.

Table XVIII. Plateau Voltages of NiO Electrodes in $PC/LiClO_4$

Current Density (mA/cm^2)	Compaction Pressure (psi)	Al (%)	Li (%)	Plateau Voltage
0.04	13,600	5	0	0.55
0.40	13,600	40	2	0.60
0.40	13,600	20	2	0.50
0.40	13,600	20	4	0.45
0.40	100,000	20	2	0.45

Although CuO exhibited a well-defined discharge plateau of 1.27 V versus Li/Li^+ (Fig. 4), its potential was also significantly below the thermodynamic value of 2.22 V. In general, the results observed indicate that the discharge of the metallic oxides does not proceed directly as written in reaction (7).

2. Metallic carbonates

Reasonable coulombic capacities were obtained from $NiCO_3$, $CoCO_3$ and basic cupric carbonate ($CuCO_3$ $Cu(OH)_2$). Although the open circuit values for the cell voltages were comparable to the thermodynamic values, polarizations were again high during discharge. Unlike the oxides, the carbonates exhibited sloping plateaus, suggesting a relatively complex discharge process. These materials were not considered further.

3. Metallic cyanides

Of the 6 cyanides tested, only AgCN and CuCN exhibited reasonable coulombic utilizations and practical cell voltages. $Ni(CN)_2$, while possessing the most attractive energy density, was electrochemically inactive. In some respects the cyanides are analogous to the chloride materials currently used in high rate

primary lithium cells. At this point, however, it was hoped that although the cyanides possess significantly lower energy densities than the corresponding chlorides, viz. 502 Whr/lb for $CuCl_2$, their solubility problems would be more manageable.

In the case of CuCN, preliminary exploration of this area was encouraging. As shown in Fig. 10, successive half-cell discharges of several CuCN electrodes over a range of current densities indicated comparable utilizations of 50 to 60%. These studies were supplemented by the discharge of a CuCN electrode which was stored in an excess of electrolyte for 48 hr prior to discharge. As can be seen in Fig. 7, no capacity loss due to CuCN dissolution was observed.

During these studies, 6 CuCN electrodes were discharged in the same electrolyte. Midway in the test regime, dark colloidal particles were seen floating off the positives. This material settled out on the bottom of the cell. However, the effect was not observed for all electrodes that were discharged.

In the case of AgCN, successive half-cell discharges analogous to those performed for CuCN indicated that electrode performance deteriorated rapidly as the result of successive discharges in the same electrolyte. Typically, the second electrode tested yielded less than 30% of the capacity of the first electrode discharged in the electrolyte. Accordingly, full-cell testing of the cyanide electrodes emphasized CuCN

B. Full-Cell Testing of CuCN Electrodes

In order to evaluate possible solubility problems arising from its discharge products, CuCN electrodes were prepared and assembled into polyethylene bag cells identical to those used previously. The electrolyte was PC/$LiClO_4$. The CuCN electrodes contained 6 g of active material (1.8 Ahr) and were 1.75 in. in diameter. All discharges were at 1 mA/cm^2 (30 mA).

Initially, the electrodes were constructed by admixing 20% Al with the CuCN. The mix was then pressed on an aluminum expanded metal grid with a spot-welded aluminum tab. Discharge of these electrodes resulted in failure after 1 to 2 hr. Postmortem of the cells showed penetration of the cell separator by copper metal. The lithium negatives were heavily contaminated with copper. In addition, heavy corrosion of the aluminum tab/grid assembly was noted, presumably due to displacement of the aluminum by copper present in the solution.

After these initial failures, copper materials were substituted for the aluminum in the positive electrode. Here again, the cells failed via copper deposition after

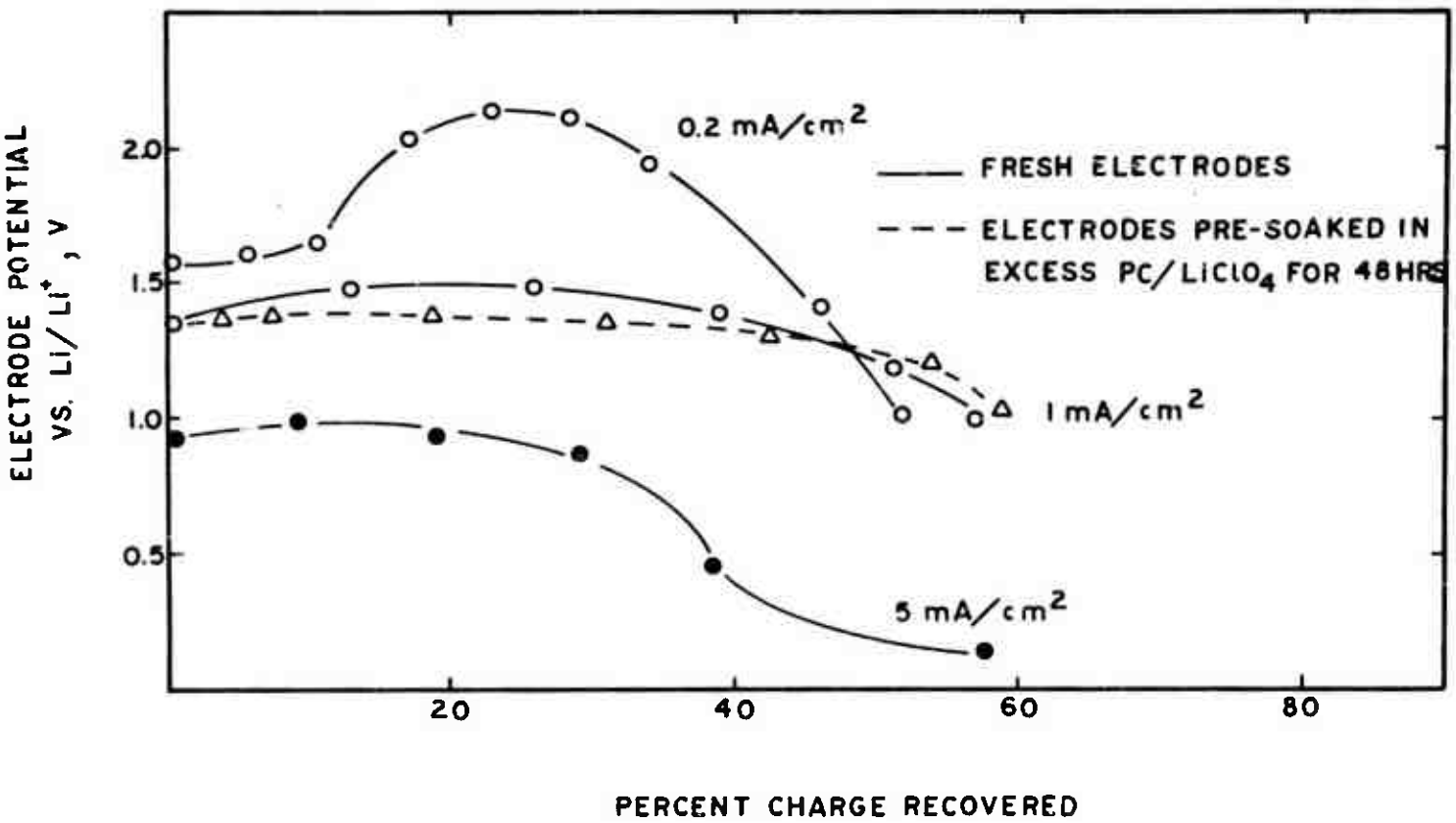

Fig. 10. Half-cell discharge performance of CuCN electrodes

only 1 to 2 hr. Attempts were then made to saturate the electrolyte with cyanide ion in order to depress the obviously high solubility of CuCN. The electrolyte from a failed cell was filtered to remove suspended copper and copper cyanide particles and then used in a new cell constructed with fresh electrodes. No improvement was noted, even after this replacement cycle was repeated three times with the same electrolyte.

It was thus concluded that the high solubility of CuCN results from a complexation mechanism analogous to that present in the discharge of chloride containing cathodes. Although the solubility of CuCN in PC/$LiClO_4$ is apparently quite low (see Fig. 7), formation of the soluble higher cyanides apparently occurs during discharge of the electrodes in relatively limited quantities of electrolyte.

Since CuCN possesses a less attractive energy density than $CuCl_2$, further study of the material was not performed.

APPENDIX A

SYNTHESIS AND CHARACTERIZATION OF BULK Ni_3S_2

An alloy of Ni-37 atomic % S was synthesized using pieces of high purity Ni wire and 99.999% sulfur powder. An earlier alloy of stoichiometric composition had been synthesized using high purity Ni powder. This alloy apparently showed evidence of the Ni_7S_6 compound, which was undesirable. It also had a oxide content which apparently resulted from the oxygen on the surface of the Ni powder.

The Ni wire was first pickled in a HNO_3-H_2O acid bath (50:50), washed thoroughly, soaked in acetone, and dried. After weighing the elements, the charge was placed in a thick-walled quartz ampoule, evacuated to 5×10^{-6} torr, and sealed off.

The ampoule was placed into a horizontal furnace at a low temperature (approximately 200°C). After the sulfur was molten, the ampoule was rotated for a short period to ensure that the molten sulfur was thoroughly wetting the Ni wire. The furnace was turned up to 500°C for a 24-hr period and then to 600°C for another day prior to actual melting. This was done in order to get the sulfur well infiltrated into the Ni wire.

The furnace was then turned up to 875°C to melt the alloy and allowed to remain at that temperature overnight. The ampoule was removed quickly from the furnace and positioned vertically in order that the molten alloy would cast as a solid rod. In order to further consolidate the alloy, the sample was remelted with the ampoule in a vertical position using an oxyacetylene torch.

The cast ingot of Ni-37 S was removed from the ampoule. A small piece from the top of the casting was broken off for X-ray diffraction analysis; the remainder of the rod was sealed off again in an evacuated Pyrex ampoule and heat-treated at 475°C for 5 days to ensure the low-temperature Ni_3S_2 polymorph (transition temperature = 530°C for this alloy composition).

X-ray diffraction analyses of both the as-melted and heat-treated portions of the Ni-37 S ingot showed the presence of the low temperature hexagonal form of Ni_3S_2, as well as some excess Ni. Since the low temperature form is the equilibrium structure of the compound and the high temperature polymorph is not quenchable,* the heat-treatment of any further Ni_3S_2 ingots is not necessary after casting, unless recrystallization or grain growth is desired.

A metallographic cross section of the heat-treated Ni-37 S alloy is shown in Fig. A-1. The major portion of the alloy is Ni_3S_2. The small white islands are the Ni solid solution phase; some porosity is also evident in the microstructure.

In a subsequent preparation, another alloy with the composition Ni-39 atomic % S was synthesized according to the same technique as described above. As a final step to this synthesis, the cast alloy was placed in a vertical furnace, remelted to 375°C, and then lowered at approximately 0.5 cm/hr into a cooler furnace zone below the solidus temperature of the alloy. This is a modification of the Bridgman technique for single crystal growth and was done with the intention of removing porosity and gas inclusions from the ingot. From initial inspection, the results did not appear to be successful for this run. Preliminary X-ray diffraction results again indicated the presence of hexagonal Ni_3S_2 with a good probability of some excess Ni.

* G. Kullerud and R. A. Yund, "The Ni-S System and Related Minerals," J. Petrology, 3 (1962) 126-175.

Fig. A-1. Metallographic cross section of heat-treated Ni-375 alloy